Estimating System State During Human Walking With a Powered Ankle-Foot Orthosis

David Yifan Li, *Student Member, IEEE*, Aaron Becker, *Student Member, IEEE*, Kenneth Alex Shorter, Timothy Bretl, *Member, IEEE*, and Elizabeth T. Hsiao-Wecksler, *Member, IEEE*

***Abstract*—This paper presents a state estimator that reliably detects gait events during human walking with a portable powered ankle-foot orthosis (AFO), based only on measurements of the ankle angle and of contact forces at the toe and heel. Effective control of the AFO critically depends on detecting these gait events. A common approach detects gait events simply by checking if each measurement exceeds a given threshold. Our approach uses cross correlation between a window of past measurements and a learned model to estimate the configuration of the human walker, and detects gait events based on this estimate. We tested our approach in experiments with five healthy subjects and with one subject that had neuromuscular impairment. Using motion capture data for reference, we compared our approach to one based on thresholding and to another common one based on k-nearest neighbors. The results showed that our approach reduced the RMS error by up to 40% for the impaired subject and up to 49% for the healthy subjects. Moreover, our approach was robust to perturbations due to changes in walking speed and to control actuation.**

***Index Terms*—Ankle-foot orthosis (AFO), cross correlation (CC), event detection, gait, state estimation.**

I. Introduction

GAIT is a cyclic task characterized by repetitive events, and is defined from the initial ground contact of the foot to the subsequent contact of the same foot. Gait events are used to divide the cycle into phases and subphases each with a functional objective that contributes to one of three main functional tasks during gait: weight acceptance (stance), support and propulsion (stance), and limb advancement (swing) [1]–[3]. Gait can be impaired by conditions including trauma, incomplete spinal cord injuries, stroke, multiple sclerosis, muscular dystrophies, polio, or cerebral palsy [1]. These deficiencies create impairments because they prevent or hinder the functional tasks required for gait.

Ankle-foot orthoses (AFOs) are orthotic devices used to correct gait deficiencies created by impairments to the lower limbs. In the U.S. alone, sizable populations exist with symptoms that can be treated with an AFO: stroke (4.7M), polio (1M), multiple sclerosis (400K), spinal cord injuries (200K) and cerebral palsy (100K) [4]. Clinically prescribed AFO systems assist impaired individuals by providing support for the lower leg and foot while restricting unwanted motion of the foot in a predetermined and fixed manner [5]–[8]. Unfortunately, these fixed motion control properties can impede gait and cannot adapt to a changing environment [9]. Powered AFO systems address the limitations of passive devices by using computer control to vary the compliance, damping, or net power of the device for motion control and torque assistance at the ankle joint [9]–[12].

The performance of a powered AFO depends critically on the ability to do two things: first, detect gait events based on measurements from onboard sensors (e.g., accelerometers, potentiometers, and force sensors), and second, control applied torque to meet the functional objective determined by each gait event. Our focus in this paper is on the first of these things, reliable detection of gait events.

Many state-of-the-art AFOs detect gait events simply by checking if each sensor measurement at a particular time exceeds a given threshold [9]–[18]. This approach has been used to provide appropriately timed motion control and torque assistance both for level walking and for stair climbing. However, this approach becomes less reliable when the individual's gait pattern changes, for example as the result of impairment, fatigue, preference, or functional assistance from the orthosis. Moreover, this approach may not even be possible when there exists no unambiguous mapping from sensor measurements to a gait event of interest, in particular an event other than "heel strike" or "toe off." These situations limit the number and reliability of gait events that can be used for control.

In this paper, we consider an alternative approach that uses the time history of sensor measurements to compute an estimate of body configuration and then detects gait events based on this estimate. It is well known that body configuration during cyclic gait can be approximated by a single state variable, the "percent gait cycle," and that gait events are associated with particular values of this state variable [1]. Recent work has shown that it is possible to compute an estimate of this state variable by

Manuscript received November 14, 2010; revised March 18, 2011; accepted June 1, 2011. Date of publication August 15, 2011; date of current version August 30, 2011. Recommended by Guest Editor E. Burdet. This work was supported in part by the National Science Foundation Engineering Research Center for Compact and Efficient Fluid Power under Grant 0540834 and in part by the National Science Foundation under Grants 0955088 and 0931871.

D. Y. Li and E. T. Hsiao-Wecksler are with the Department of Mechanical Science and Engineering, University of Illinois at Urbana-Champaign, Urbana, IL 61820 USA (e-mail: yifanli4@illinois.edu; ethw@illinois.edu).

A. Becker is with the Department of Electrical and Computer Engineering, University of Illinois at Urbana-Champaign, Urbana, IL 61820 USA (e-mail: abecker5@illinois.edu).

K. A. Shorter was with the Department of Mechanical Science and Engineering, University of Illinois at Urbana-Champaign, Urbana, IL 61820 USA. He is now with Woods Hole Oceanographic Institution, Woods Hole, MA 02543 USA (e-mail: shorter2@illinois.edu).

T. Bretl is with the Department of Aerospace Engineering, University of Illinois at Urbana-Champaign, Urbana, IL 61820 USA (e-mail: tbretl@illinois.edu).

Color versions of one or more of the figures in this paper are available online at http://ieeexplore.ieee.org.

Digital Object Identifier 10.1109/TMECH.2011.2161769

comparing motion capture data (producing measurements of lower-limb joint angles and joint velocities) to a learned model [19]. We will do the same, but must address the fact that a powered AFO typically does not have access to motion capture data, nor to similarly rich sensor measurements.

In particular, our approach computes a state estimate (i.e., an estimate of where an individual is in the gait cycle) based only on measurements of the ankle angle and of contact forces at the toe and heel. These measurements are taken only from sensors mounted on the portable powered AFO (PPAFO) that we use in our experiments [18]. This sensor package is comparable to what is found on other AFOs, including those of Blaya and Herr [10] with joint angle and ground reaction force sensors, Svensson and Holmberg [9] with a joint angle sensor, and Hollander *et al.* [15] with a joint angle sensor and foot switches. None of these sensor packages are sufficient to compute a state estimate based only on one set of measurements. However, due to the cyclic nature of gait, sensor measurements from different gait cycles exhibit a high degree of correlation. We take advantage of this fact to compute a state estimate based on maximizing the cross correlation (CC) between a window of past sensor measurements and a reference model learned from training data. When tested in experiments with human subjects, our approach to event detection was more accurate and more robust to changes in gait than other approaches previously reported in the literature.

A. Overview

Throughout this paper, we will denote time by $t \in \mathbb{R}$, the state variable describing percent gait cycle by $\lambda \in [0, 100)$, and the vector of sensor measurements by $\mathbf{y} \in \mathbb{R}^3$. Since the mapping from λ to gait events is well known [1], our goal is to compute an estimate $\hat{\lambda}(t)$ of the state $\lambda(t)$ at the current time t based on all sensor measurements $\{\mathbf{y}(s) | s \in [0, t]\}$ up to this time. In our experiments, we use the method of [19] to compute a reference estimate $\lambda^*(t)$ based on motion capture data, and define the error in our own estimate by $\lambda_{\mathrm{err}}(t) = \hat{\lambda}(t) - \lambda^*(t)$.

To examine the performance of our proposed CC estimator, we compare it to two other estimators and to a direct event (DE) detector. All three estimators that we consider are based on a precomputed model $\bar{\mathbf{y}}(\lambda)$ that tells us what sensor measurements to expect at a given state λ. This model is given by regression analysis of training data $(\lambda^*, \mathbf{y})$. We also derive the average cycle period T from this model. The estimators and DE detector are as follows:

1) *CC:* The estimate $\hat{\lambda}_{\mathrm{CC}}$ minimizes the sum-squared error between sensor readings from the last T seconds and training data with a phase shift of $\hat{\lambda}_{\mathrm{CC}}$.
2) *k-nearest neighbors (kNN):* The estimate $\hat{\lambda}_{k\mathrm{NN}}$ minimizes the squared error between the current sensor reading and training data at $\hat{\lambda}_{k\mathrm{NN}}$.
3) *Fractional time (FT):* The estimate $\hat{\lambda}_{\mathrm{FT}}$ is the time since the last heel strike (determined by thresholding the heel sensor) normalized by T.

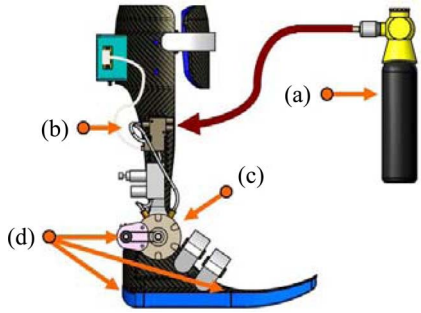

Fig. 1. PPAFO system components. (a) Power supply: a compressed CO_2 bottle with regulator provides up to 120 lbf/in^2 for the system. (b) Valves: two 3-2 solenoid valves control the flow of CO_2 to the actuator. (c) Actuator: a pneumatic rotary actuator provides up to 12 N·m at 120 lbf/in^2. (d) Sensors: two force sensors under the heel and toe and a potentiometer at the ankle joint.

4) *DE:* DE uses thresholds on heel and toe sensors to determine heel strike and toe off events. Because DE is limited to these two events, it is not a state estimator.

FT is similar to what is found in the AFO literature [9]–[18], kNN is similar to [19] but applied to AFO sensor data rather than motion capture data, and CC is the approach that we present here. We emphasize that CC is a classical method of signal processing (e.g., [20]) that has been used previously for gait analysis (e.g., [21], [22]). Our contribution is the application of this approach to state estimation for a powered AFO and the analysis of experiments with human subjects necessary to demonstrate its performance.

The remainder of our paper proceeds as follows. Section II describes the experimental methods used to quantify the performance of each state estimator. Section III presents the details of our CC state estimator and two others used as a basis for comparison. Section IV provides the results of experiments with five healthy subjects and one subject that had neuromuscular impairment. Section V considers the implications of these results in the context of AFO control. Section VI gives concluding remarks.

II. Experimental Methods

Three state estimators (CC, kNN, and FT) and DE were implemented on a powered AFO capable of operation in real-world environments outside of the laboratory or clinic. A reference estimate λ^* was also derived using kinematic data from a motion capture system and kinetic data from an instrumented treadmill. Experimental trials with five healthy subjects and one subject with a neuromuscular impairment were performed to assess the three AFO estimators on their performance relative to the reference state model λ^*, ability to identify relevant gait events during the cycle, and robustness to speed and actuation perturbations. This section describes the PPAFO system, the gait lab data collection procedure, and the experimental setup.

A. Powered Orthosis System

The PPAFO in this paper used a pneumatic power supply and a rotary actuator at the AFO ankle joint for motion control and propulsion assistance, (see Fig. 1) [18]. The PPAFO control loop and estimators ran at 66 Hz, using sensor feedback sampled at

the same rate from two force sensors (0.5 in circle, Interlink Electronics, Camarillo, CA) mounted underneath the heel and toe between the carbon fiber shell and the sole of the PPAFO and a potentiometer (53 Series, Honeywell, Golden Valley, MN) that measured the angle between the shank and foot sections.

B. Experimental Setup and Pretest Procedures

1) Experimental Setup: Subjects walked with the PPAFO on an instrumented treadmill. For each trial, the subject wore sleeveless top and snug-fitting shorts. Thirty two reflective markers were attached to the body, including torso, thighs, shanks, feet, and the PPAFO. Data from the healthy subject were collected at the University of Illinois, Urbana-Champaign, Urbana. Kinematic data were collected using a six-camera motion capture system sampled at 150 Hz (Model 460; Vicon, Oxford, U.K.). Ground reaction force (GRF) data for each foot was collected on a split-belt treadmill with embedded force plates sampled at 1500 Hz (Bertec, Columbus, OH). Data from the impaired subject were collected at Georgia Institute of Technology, Atlanta. Kinematic data were collected using a six-camera system sampled at 120 Hz (Model 460; Vicon, Oxford, U.K.). The kinetic data were collected on a custom force-sensing instrumented split-belt treadmill sampled at 1080 Hz [23]. Joint angles were calculated from kinematic data. Joint angles and GRF were filtered by a low-pass, fourth-order, zero-lag, Butterworth filter with cutoff frequency of 10 Hz. All procedures were approved by the institutional review boards of the University of Illinois and Georgia Institute of Technology, and all participants gave informed consent.

2) Subject Information:

a) Healthy Subjects: The five healthy male subjects (28 ± 4 years; height 186 ± 5 cm; mass 72 ± 8 kg) had no gait impairments and no history of significant trauma to the lower extremities or joints.

b) Impaired Subject: The impaired male subject (51 years; height 175 cm; mass 86 kg) has a diagnosis of *cauda equina syndrome* caused by a spinal disk rupture. This gait deficit does not allow him to generate plantarflexor torque to push his toes down. The subject walks without the use of walking aids (i.e., cane or walker), but usually wears AFOs bilaterally. For our testing, he wore his own prefabricated carbon composite AFO (Blue RockerTM, Allard, NJ) on his left leg while walking with the PPAFO on his right leg.

3) Determining Self-Selected Speed: A self-selected walking speed for each subject was determined prior to testing. For the healthy subjects, comfortable treadmill walking speed was determined by averaging three self-selected speeds chosen while wearing the PPAFO with no actuation. Average walking speed for the five healthy subjects was 1.18 ± 0.11 m/s with an average gait period of 1.16 ± 0.09 s over 30 s of walking. The impaired subject's comfortable walking speed was determined while in his running shoes on the treadmill with no assistive devices on either leg. This walking condition was used because it was the impaired subject's most difficult condition. Walking speed for the impaired subject was 0.7 m/s with an average gait period of 1.09 ± 0.04 s over 30 s of walking.

C. Training Data for Estimation Models

The PPAFO state estimators require a model derived from data collected during a preliminary training process. Each model is unique to each subject, and is not varied between experimental trials. During this process, a subject walked with the unactuated PPAFO on the treadmill for 30 s at his comfortable walking speed.

GRF_Z data from the force-sensing treadmill were compared to a threshold to identify heel strikes. The average period of the gait cycle T was calculated from these data.

The data were also used to create regression models for each of the PPAFO sensor measurements during gait cycles. Models for different sensors were computed separately. Each model is a function of cycle state λ, where $\lambda \in [0, 100)$, and describes the expected reading for a given sensor $\bar{y}(\lambda)$. The regression models were formulated in the following manner.

For each sensor, we use locally weighted regression analysis [24] to establish the functional relationship between the normalized input/output pairs of state λ and sensor measurement y

$$(\lambda_1, y_1), \ldots, (\lambda_N, y_N)$$

where N is the number of measurements collected from training, and λ is the percent gait cycle found by normalizing time between heel strikes.

Regression evaluates $\bar{y}$ at the point λ. This evaluation depends on the signed distance

$$x_i = \mathrm{dist}(\lambda_i - \lambda)$$

between λ_i and the query point λ. Because λ_i and $\lambda \in [0, 100)$, the distance is defined as

$$\mathrm{dist}(\lambda_i - \lambda) = \begin{cases} (\lambda_i - \lambda) - 100 & \text{if } \lambda_i - \lambda > 50 \\ \lambda_i - \lambda & \text{if } -50 \leq \lambda_i - \lambda \leq 50 \\ (\lambda_i - \lambda) + 100 & \text{if } \lambda_i - \lambda < -50. \end{cases}$$

First, we select a fixed set of M polynomial basis functions

$$\phi(x_i) = \left[1, x_i, \ldots, x_i^{M-1}\right]^T$$

and denote

$$\Phi = \begin{bmatrix} \phi(x_1)^T \\ \vdots \\ \phi(x_N)^T \end{bmatrix}.$$

We also define

$$Y = \begin{bmatrix} y_1 \\ \vdots \\ y_N \end{bmatrix}$$

by concatenating the data associated with each output. We select the row vector $v \in \mathbb{R}^M$ of parameters that minimizes the weighted sum-squared error e

$$e = \sum_{i=1}^{N} w_i \left(y_i - v^T \phi(x_i)\right)^2$$

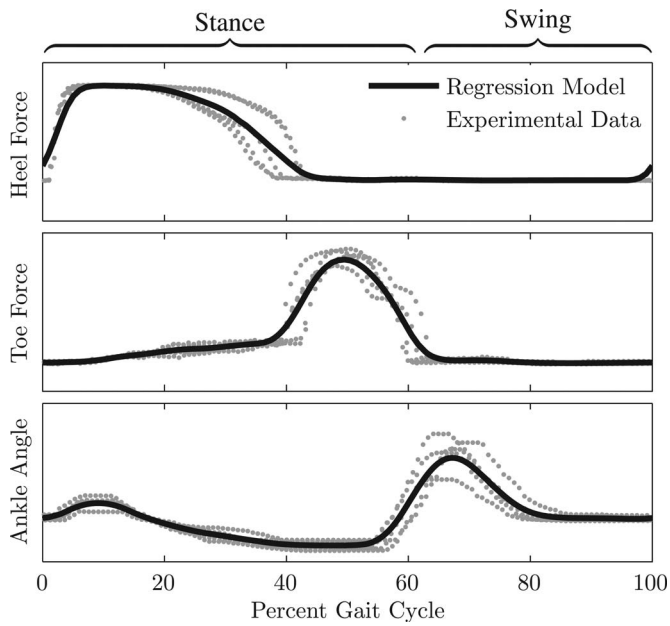

Fig. 2. Locally weighted linear regression analysis with $M = 2$ polynomial basis functions and a weighting bandwidth of $r = 0.02$ applied to heel force, toe force, and ankle angle sensor measurements as a function of percent gait cycle. Five cycles of sensor measurements (gray dots) from healthy subject #3 walking at steady state, self-selected speed were used to create a regression model $\bar{y}(\lambda)$, shown in black, for each sensor.

where

$$w_i = \exp\left(-\frac{x_i^2}{2r^2}\right), \quad \text{for each } i = 1, \ldots, N$$

and r is a design parameter. Because w_i depends explicitly on λ, we must store and use the entire set of training data $(\lambda_1, y_1), \ldots, (\lambda_N, y_N)$ to make predictions. Let

$$W = \text{diag}\,(w_1, \ldots, w_N)$$

then the cost function can be rewritten in matrix form

$$e = (\Phi v - Y)^T W (\Phi v - Y).$$

In order to minimize e, v can be solved as

$$v(\lambda) = \left(\Phi^T W \Phi\right)^{-1} \Phi^T W Y.$$

Now we can obtain the regression model for a given sensor over one gait cycle as

$$\bar{y}(\lambda) = v(\lambda)^T \phi(0).$$

For each subject, we precompute $\bar{y}(\lambda)$ at $\lambda = \{0, 1, \ldots, 99\}$ for all three sensors, and they will form the sensors regression model matrix $\bar{\mathbf{y}}(\lambda)$. The results of applying this form of regression analysis to multiple gait cycles of healthy subject #3 are shown in Fig. 2.

D. Experimental Testing Procedure

Tests were conducted with two possible disturbances: *actuation* and *slow speed*. The actuation disturbance modeled the effect of providing assistive torque with the PPAFO. During each gait cycle, a plantarflexor (toes down) disturbance torque was applied if both the toe and heel sensors were loaded, and a dorsiflexor (toes up) disturbance torque was applied if both sensors were unloaded—otherwise, no disturbance torque was applied. State estimates (from CC, kNN, or FT) could also have been used to trigger the application of torque in these experiments, but the use of a simple decision rule allowed for a less biased comparison between estimators. Fig. 3 shows the resulting change in gait kinematics as a consequence of actuation. The slow speed disturbance modeled the effect of variable walking speed, which is a common gait perturbation. It was created by slowing the treadmill.

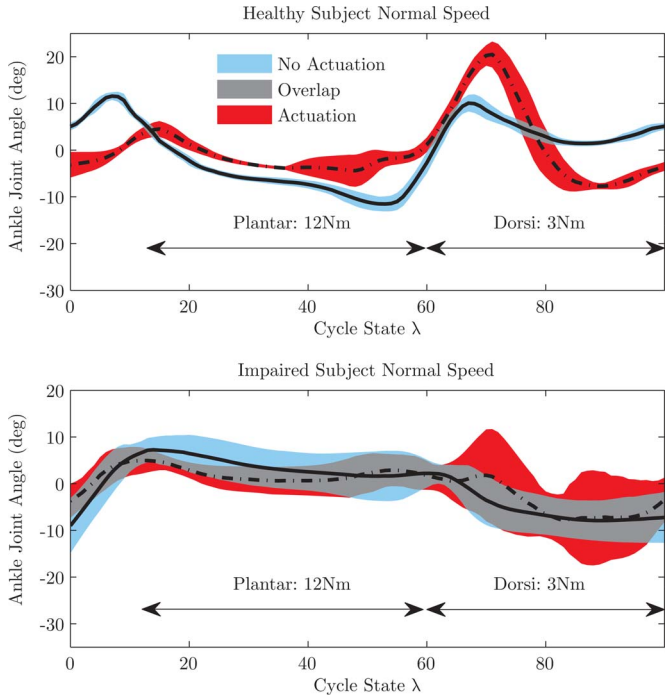

Fig. 3. (Top) Ankle joint angle for healthy subject #3 and (Bottom) the impaired subject with and without actuation at normal speed. The PPAFO was able to generate a modest plantarflexor torque (12 N·m) compared to a healthy walker (105 N·m for a 70 kg individual). Only 3 N·m of dorsiflexor torque was required to support the foot during swing. Sensor readings without actuation and with actuation are significantly different. Because the sensor regression model was generated without actuation, these differences resulted in worse correlation between current measurements and the model. For the impaired subject, excessive dorsiflexion actuation during swing may have caused the large variability of ankle joint position.

Five experimental trials were used to evaluate the performance of the PPAFO estimators under these two disturbances. For each test, the subjects were given time to reach a steady walking speed on the treadmill before data collection began. Thirty seconds of data were recorded during steady-state walking for trials 1–4.

1) Normal Speed—No Actuation (Healthy and Impaired): This test compares the PPAFO estimators under nominal conditions. Each subject walked at his self-selected speed (normal speed) with no actuation from the PPAFO.

2) Normal Speed—Actuation (Healthy and Impaired): Torque applied by the PPAFO can affect gait timing and sensor readings, adversely impacting estimation. The PPAFO was

supplied with pneumatic power at 110 lbf/in^2 and actuated by the simple threshold rule described earlier.

3) Slow Speed—No Actuation (Healthy and Impaired): The treadmill was set to 75% of the subject's self-selected speed, with no PPAFO actuation.

4) Slow Speed—Actuation (Healthy and Impaired): This trial examined the effects of slow walking (75% of self-selected speed) along with actuation. The actuation was in the same manner as trial 2 earlier.

5) Change in Speed (Healthy): Changing speed is a common gait perturbation. A speed change was introduced to examine the effect of this perturbation on the accuracy of the PPAFO estimators. Each healthy subject began walking at his self-selected speed. After 20 s, the treadmill was gradually slowed to 75% of self-selected speed in approximately 5 s. The speed remained 75% of self-selected speed for the rest of the trial. Sixty seconds of data were recorded during the trial.

E. Estimation Comparison Metrics

Two metrics were used to evaluate and compare the performance of the PPAFO estimators for the tests in Section II-D.

1) *Event Detection*: Temporal errors were compared between gait event times identified using gait lab data, event times predicted by the three PPAFO estimators, the DE detector, and the reference state estimator λ^*. The gait events selected for comparison were right heel strike, left toe off, left heel strike, and right toe off.
2) *State Estimation*: Errors were compared between reference state estimate λ^* and the three PPAFO state estimates throughout the cycle.

III. State Estimation Techniques

The experiments described in the previous section tested three state estimators (CC, FT, and kNN) and the DE detector, all based on PPAFO sensor measurements in comparison to a reference estimate λ^* based on motion capture and treadmill data. In this section, we will describe how each state estimator was implemented.

A. Estimate Based on CC

The CC estimator slides a window of actual sensor data across the regression model of the sensor data, and finds the point where the mean-square-error is minimized (i.e., where the data and model best align). Given the regression model $\bar{\mathbf{y}}$ and the average period T, we can apply the CC approach to estimate λ at each time t. We do this in the following way. We have precomputed $\bar{\mathbf{y}}[\lambda]$ at $\lambda = \{0, 1, \ldots, 99\}$ using the aforementioned locally weighted linear regression approach. We take a time history of sensor data $\mathbf{y}_1, \ldots, \mathbf{y}_m$ sampled at m particular times $t_1, \ldots, t_m \in [t - T, t]$. For all $j = 1, \ldots, m$, we normalize these times according to

$$\lambda_j = 100 \left(\frac{t_j - (t - T)}{T} \right)$$

then generate an index set $I = I_1, \ldots, I_m$ according to

$$I_j = \text{round}\,(\lambda_j)$$

so that each I_j will be an integer index between 0 and 100. We denote the measurements by $\mathbf{y}[j] = \mathbf{y}_j$. We wrap the regression model around periodic borders by setting $\bar{\mathbf{y}}[i] = \bar{\mathbf{y}}[i \pm 100]$ for all i. The state estimate $\hat{\lambda}_{\text{CC}}$ is the integer $k \in \{0, \ldots, 99\}$ that minimizes

$$\sum_{j=1}^{m} \left(\bar{\mathbf{y}}[I_j + k] - \mathbf{y}[j]\right)^T \left(\bar{\mathbf{y}}[I_j + k] - \mathbf{y}[j]\right).$$

B. Estimate Based on FT

The FT estimator assumes that the state estimate $\hat{\lambda}$ increases linearly with time from heel strike

$$\hat{\lambda}_{\text{FT}} = 100(t - t_{\text{hs}})/T$$

where t_{hs} is the time of last heel strike as determined by thresholding $\mathbf{y}(t_{\text{hs}})$, and T is the average cycle period.

C. Estimate Based on kNN

Another common way to estimate state is to compute the best match between current sensor measurements $\mathbf{y}$ and the regression model learned from training data $\bar{\mathbf{y}}$

$$\hat{\lambda}_{k\text{NN}} = \underset{\lambda \in [0,100)}{\arg\min} \; \|\mathbf{y}(t) - \bar{\mathbf{y}}(\lambda)\|_2.$$

This approach can be improved by averaging the k best matches ("kNN" [25]). We chose $k = 3$.

D. Reference Estimate λ^*

We use an estimator generated from motion capture and treadmill data as a reference for comparing the PPAFO estimators. The joint angle information expands eight variables (vertical ground reaction forces, and bilateral hip, knee, and ankle angles) and their derivatives to a 16-D state space. We build a linearly weighted regression model $\bar{\mathbf{q}}$ using data from multiple cycles to form a closed curve in this 16-D state space. This curve is divided into 100 sections and labeled linearly with time. λ^* is the label of the nearest neighbor on the curve to the current measurement vector, as in [19].

At time t, the sensors return a 16-element vector $\mathbf{q}(t)$. We compare this vector to the regression model $\bar{\mathbf{q}}$. The state λ^* at time t is defined as

$$\lambda^*(t) = \underset{\lambda \in [0,100)}{\arg\min} \; \|\mathbf{q}(t) - \bar{\mathbf{q}}(\lambda)\|_2.$$

Fig. 4 illustrates how normalizing the data by λ^* aligns sensor measurements across different trials better than by time or percent gait cycle.

IV. Results

CC and FT outperformed kNN for all tests. For the impaired subject, CC demonstrated the best accuracy for all tests, reducing event detection RMS error by up to 40% compared to FT. For the healthy subjects, FT and CC performed comparably during

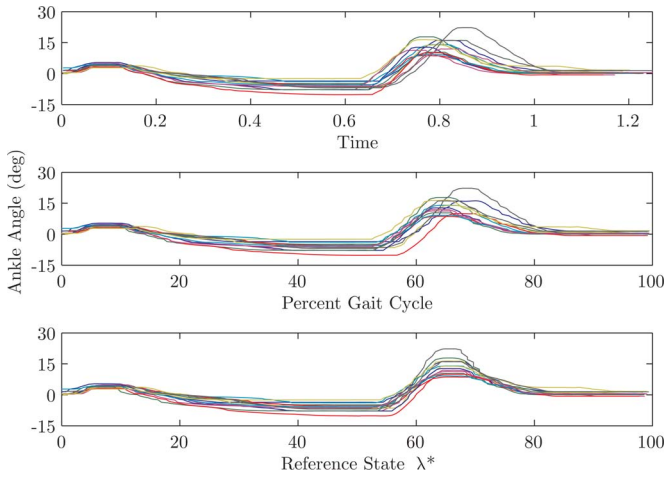

Fig. 4. Ankle angles of healthy subject #3 aligned at heel strike for ten cycles. The angle is plotted with respect to time, percent gait cycle, and reference estimate λ^*.

normal speed walking, but CC was more accurate during slow walking tests (see Tables I and II).

1) Normal Speed—No Actuation (Healthy and Impaired): For the healthy subject, both CC and FT worked well for event detection and state estimation, while kNN did not. FT had low state estimate error around heel strike, but the error increased as time progressed in the gait cycle [see Fig. 5(a)] while CC stayed relatively low. For the impaired walker, the CC technique had a smaller average error (see Figs. 5(b) and 6). The FT estimate diverged more during swing [see Fig. 5(b)].

2) Normal Speed—Actuation (Healthy and Impaired): This task verified that FT and CC can successfully track the system state, even when actuated. The RMS error for state estimate is under 4% for the healthy subjects and around 10% for the impaired subject. For the healthy subjects, FT and CC have similar performance, with FT having slightly higher accuracy. CC for the impaired subject has 23% lower RMS error than FT, a decrease in RMS state error from 12.4 to 8.0 (see Table II).

3) Slow Speed—No Actuation (Healthy and Impaired): For the healthy subjects, this test shows the largest improvements of CC over FT in both event detection and state estimate error. For both healthy and impaired subjects, the CC reduced the state estimate error by at least 29%, from 10 to 7.1 and the event detection error by at least 30%, from 69.6 to 49.4 ms (see Tables I and II).

4) Slow Speed—Actuation (Healthy and Impaired): The combined speed and actuation perturbations make this the only test where kNN becomes competitive with other estimators. The healthy subjects were best estimated using CC. For the healthy subjects, the state estimate RMS error was reduced 25% from FT to CC. For the impaired subject, the results are striking: a 40% reduction in state estimate error from FT to CC, from 15.7 to 9.6 (see Table II).

5) Change in Speed (Healthy): This test reduced the walking speed by 25% midway through the trial. Fig. 7 shows the errors from the three estimators as a function of overall time for this test. The error variance for FT illustrates unreliability at the slower walking speed, while CC maintains accuracy. The RMS and worst case for FT were all reduced by a factor of two by the CC estimate.

V. Discussion

We have presented a new method of state estimation for powered PPAFOs (CC) that can be used to detect gait events. We also presented results from testing this method and three others (FT, kNN, and DE) in experimental trials during treadmill walking with both healthy and impaired subjects. In this section, we will discuss the performance, robustness, applications to control, and limitations of these state estimation schemes.

A. Performance During Healthy Unperturbed Gait

The CC and FT estimators performed comparably during the healthy subject normal speed walking trials. The CC estimator correlates a window of past sensor readings to a regression model of normative sensor data to estimate the state. The FT estimator is an extension of the DE estimator using thresholds, and only requires a model of subject's gait period. The FT has the advantage of simple implementation, but as we will discuss in the following, the CC estimator was more robust to disturbances.

The kNN estimator performed poorly during all subject trials. This estimator is based on [19], but uses PPAFO sensor data rather than motion capture data as in [19]. The poor performance of kNN was due to the limited data used to construct subject's state configuration, and that kNN only makes use of the current sensor measurements. This shortcoming is compounded because the PPAFO sensor data contain large sections with nearly identical readings (see Fig. 2, e.g., 70–100% gait cycle). As a result, kNN cannot reliably compute gait state during these periods.

B. Robustness To Speed and Actuation Disturbances

The robustness of the estimators was evaluated during trials with speed and actuation disturbances. A decrease in speed was used to perturb gait because preliminary experimentation demonstrated greater estimation errors after a decrease rather than an increase in speed. Future work could examine the robustness of the CC estimator by applying time varying disturbances such as sinusoidal speed variations, accelerations/decelerations, and gait initiation/cessation. A simple decision rule, rather than using the state estimators, was used to determine the timing of the actuation disturbance to allow for an unbiased comparison. This approach enabled the performance of the individual estimation schemes to be evaluated in the presence of the same disturbances. Our use of the term "actuation disturbance" may seem unusual, since the nominal purpose of the PPAFO is to provide assistance with applied torque. However, by choosing to view applied torque as a disturbance, we are hoping to ensure that estimators perform well regardless of the control policy used.

On average, the speed disturbance increased the estimation error by a factor of 2.4 for healthy subjects and 1.9 for the impaired subject, and the actuation disturbance increased the

TABLE I
EVENT DETECTION ERROR RESULTS FOR EACH TECHNIQUE DUE TO SPEED AND ACTUATION PERTURBATION EFFECTS FOR HEALTHY AND IMPAIRED SUBJECTS

5 Healthy Subjects						*Impaired Subject*					
Actuation	Speed	Method	RMS Error (ms)	Ave. Error (ms)	Worst (ms)	Actuation	Speed	Method	RMS Error (ms)	Ave. Error (ms)	Worst (ms)
0psi	Normal	CC	**14.8±4.8**	-1.7±2.9	35.5±19.1	0psi	Normal	CC	**36.8**	-3.6	**76.7**
		FT	14.8±5.6	**1.7±1.5**	**30.5±9.7**			FT	53.2	-1.4	138.2
		kNN	65.0±29.0	-14.8±9.6	208.1±194.3			kNN	104.6	**-1.4**	441.6
		λ^*	6.4±1.2	-1.2±2.0	14.7±3.0			λ^*	19.0	-6.2	33.3
		DE†	5.8±2.8	2.3±2.0	13.2±6.8			DE†	39.1	3.0	78.2
110psi	Normal	CC	45.9±15.0	17.0±36.7	113.8±54.8	110psi	Normal	CC	**87.6**	-64.2	**23.4**
		FT	**41.9±11.8**	27.6±15.3	**106.5±52.4**			FT	113.4	-86.0	44.1
		kNN	93.6±38.0	**1.2±26.4**	307.0±184.2			kNN	353.2	**-25.1**	762.9
		λ^*	7.6±1.4	-0.9±2.6	18.7±5.6			λ^*	15.5	0.5	57.4
		DE†	31.3±13.2	13.3±11.9	77.2±66.4			DE†	51.3	-25.8	19.2
0psi	Slow	CC	**49.4±23.9**	-29.0±25.2	**37.7±26.1**	0psi	Slow	CC	**74.8**	-47.2	**62.3**
		FT	69.6±15.7	-41.8±15.9	49.7±32.2			FT	108.8	-33.8	157.9
		kNN	77.8±32.4	**10.8±18.9**	289.7±199.0			kNN	110.9	**-5.3**	576.3
		λ^*	9.5±4.2	0.3±2.7	30.4±28.5			λ^*	18.4	-0.5	30.6
		DE†	14.2±5.1	-0.9±5.2	25.3±28.6			DE†	47.9	-8.6	78.0
110psi	Slow	CC	84.0±53.2	-51.5±52.9	**47.7±24.6**	110psi	Slow	CC	**105.5**	-81.1	**21.5**
		FT	**82.9±20.9**	-35.0±24.0	81.2±30.1			FT	175.7	-103.5	167.6
		kNN	112.7±88.7	**3.9±27.2**	272.0±190.9			kNN	214.8	**17.2**	681.9
		λ^*	16.0±18.5	7.3±13.4	33.3±29.8			λ^*	14.2	2.3	59.3
		DE†	37.9±12.6	5.9±15.5	59.8±22.4			DE†	50.2	-19.4	67.6

†The direct event detector (DE) can only detect toe off and heel strike on the right foot.
True event times for left and right heel strike and toe off events are detected using treadmill force sensors. Gait period $T = 1.16 \pm 0.09$s for healthy and 1.09±0.04s for impaired. For the healthy subjects, errors are reported as mean±1 standard deviation. The best PPAFO estimator for each case is bolded and highlighted in dark gray. DE and the reference estimate λ^* are highlighted in light gray and were not included in this comparison between estimators.

TABLE II
STATE ESTIMATION ERROR RESULTS FOR EACH TECHNIQUE DUE TO SPEED AND ACTUATION PERTURBATION EFFECTS FOR HEALTHY AND IMPAIRED SUBJECTS

5 Healthy Subjects						*Impaired Subject*					
Actuation	Speed	Method	RMS Error (λ)	Ave. Error (λ)	Worst (λ)	Actuation	Speed	Method	RMS Error (λ)	Ave. Error (λ)	Worst (λ)
0psi	Normal	CC	1.3±0.4	-0.1±0.1	4.5±1.2	0psi	Normal	CC	2.9	0.4	7.7
		FT	1.3±0.5	-0.0±0.3	4.7±1.7			FT	4.3	1.5	11.4
		kNN	6.2±1.0	0.2±0.5	34.4±9.1			kNN	12.9	-2.4	49.4
110psi	Normal	CC	3.5±1.6	-1.1±3.5	7.9±1.9	110psi	Normal	CC	8.0	7.1	18.9
		FT	3.2±0.8	-1.5±1.6	9.7±2.4			FT	12.4	11.8	25.8
		kNN	8.9±2.0	0.2±2.2	41.3±9.4			kNN	21.6	6.1	49.0
0psi	Slow	CC	3.9±1.8	2.8±2.1	13.2±8.3	0psi	Slow	CC	7.1	6.2	14.6
		FT	7.7±1.7	6.4±1.5	18.1±3.6			FT	10.0	8.2	26.4
		kNN	8.5±1.1	-2.6±1.5	37.8±7.3			kNN	10.8	-0.5	48.0
110psi	Slow	CC	7.1±3.7	5.6±4.3	13.9±5.6	110psi	Slow	CC	9.6	8.4	19.9
		FT	9.3±3.6	7.4±3.2	21.3±6.3			FT	15.7	13.7	32.0
		kNN	8.2±3.5	-0.0±1.3	25.7±13.8			kNN	15.6	-1.9	51.5

For the healthy subjects, errors are reported as mean±1 standard deviation. The best estimator for each case is highlighted. Errors are the difference between PPAFO estimators and reference estimation λ^*.

error by a factor of 2.6 for healthy subjects and 1.6 for the impaired subject.

The CC estimator was more robust to the speed perturbation and performed better during the impaired walking trials (both with and without actuation) as compared to the FT and kNN estimator (see Tables I and II). The performance of FT and CC estimators were comparable during healthy walking trials perturbed by actuation. The kNN estimator was not robust to either of the disturbances.

The CC estimator performed well during all of the perturbed walking trials. The results from the impaired subject are particularly noteworthy because these results are representative of the intended population for this assistive device. During both perturbed and unperturbed gait of the impaired subject, the CC estimator outperformed the FT estimator by a minimum state estimation RMS error of 29% and a minimum event detection error of 23% (see Tables I and II). The benefits of the CC estimator are also highlighted by the healthy walking trials with the speed perturbation, where the state estimate RMS error and event detection RMS error were up to 49% and 29% smaller than the errors resulting from the FT estimation. During the healthy walking trials with the actuation perturbation, the performance of the CC estimator was comparable to the FT estimator. Actuation perturbation introduced differences to the sensor readings with little change to the cycle period (T for 0 lbf/in^2 normal: 1.16 ± 0.09 s versus 110 lbf/in^2 normal: 1.18 ± 0.04 s). As a result, the FT estimator maintained accuracy, while the CC estimator was adversely affected by the weaker correlation between sensor measurements and the sensor regression models (see Figs. 3 and 5).

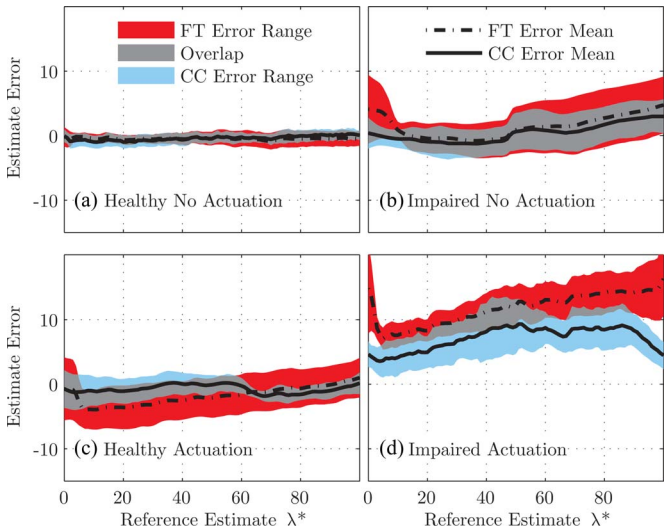

Fig. 5. Continuous state estimate error (mean and ±1 standard deviation) of FT and CC estimators and the overlap of the two behaviors for healthy subject #3 and the impaired subject, with and without actuation.

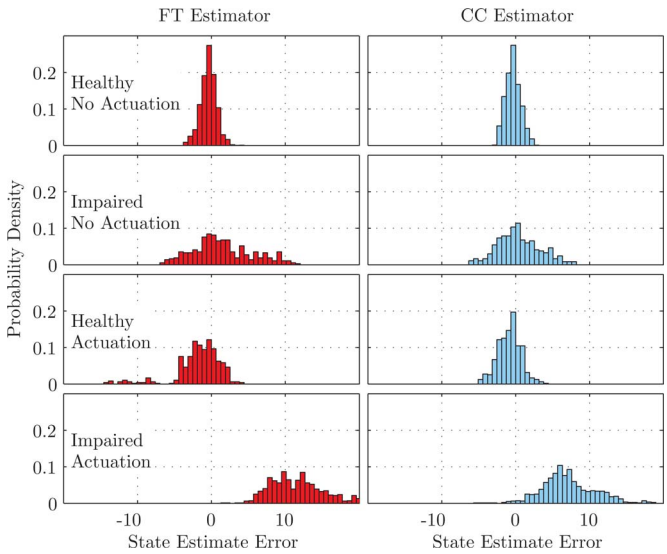

Fig. 6. Histograms of errors from FT and CC estimators for healthy subject #3 and the impaired subject, with and without actuation. The CC estimator demonstrates higher precision and often lower error, i.e., tighter distributions.

While the FT estimate performed well with the healthy walkers during normal speed walking and with actuation perturbation, this estimator was not robust to the speed perturbation. Fig. 7 clearly shows the degradation in performance of the estimator following the decrease in speed. The speed perturbation changed the cycle period, leading to a reduction in FT estimator performance because FT was dependent on a predetermined cycle period. The FT estimator did not outperform the CC estimator during any impaired walking trials.

Table I shows that DE detection RMS error was up to six times larger for the impaired subject than the healthy subjects during the normal walking trials. The increased event detection error is a significant component in the degradation of FT estimator performance for all impaired walking trials. Certain impaired

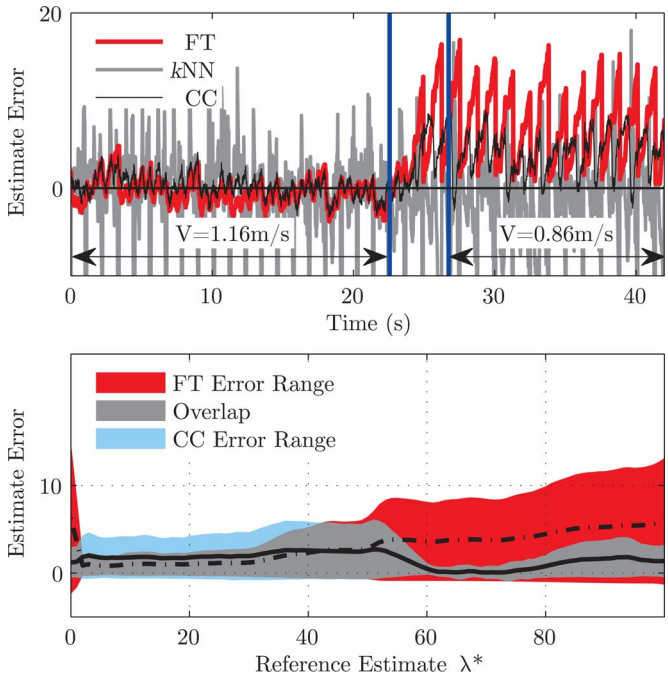

Fig. 7. Estimation error of healthy subject #3 during the change in speed test. The walking speed changed from 1.16 to 0.86m/s. (Top) Estimate error as a function of time. (Bottom) Overall estimate error as a function of state during the slow speed section. Note the high variance in the FT error at the slower speed caused by the cycle period T increasing from 1.16 ± 0.09 to 1.32 ± 0.09s.

walking patterns make event detection difficult, causing the DE estimator and any estimator relying on DE to perform poorly. In contrast, CC bases its estimate on the raw sensor measurements, not an assumed model of gait and, thus, is more robust to gait impairments.

C. Applications to Control

As we have emphasized throughout this paper, many powered AFOs rely on gait events to determine control objectives [9]–[18], and so reliable event detection is required for system control. Notable exceptions are powered orthotic systems that use surface electromyography (EMG) to directly control actuation [26]. That approach eliminates the necessity of gait event detection, but is limited by surface EMG signal reliability and availability.

In the current study, we have demonstrated that the CC estimator is able to accurately and robustly determine events during the gait cycle using data from PPAFO sensors. However, the CC estimator has broader applicability than just the PPAFO. In particular, a similar approach could be applied to provide state estimates for the control of any other assistive device (e.g., another orthosis or prosthesis) that has quasi-periodic inputs and outputs.

As we discussed in Section I, the control problem for an AFO has two parts, gait event detection and the controlled application of torque to meet the functional objective determined by each gait event. Our experiments showed the results (see Tables I and II) of using state estimators to detect gait events but did not use these detected events as the basis for controlling torque.

Future work will evaluate PPAFO performance during walking trials when state estimates (in particular, those provided by CC or FT) are used to control the actuation timing.

D. Current Limitations

The key limitation of our current approach to state estimation is that it requires a preliminary training process. This process was necessary to construct models used for state estimation. Inaccuracies in the CC estimate were created by mismatched training and actual testing conditions. One approach to reduce these inaccuracies would be to parameterize the models with respect to other gait variables such as gait period T. In this scenario, gait period would be measured directly from one of the sensors (e.g., heel sensor) and used to select the appropriate model from a library of predetermined models in real time. The training process was also time consuming and could serve as an impediment for use in a clinical setting. This issue could be addressed by continuously updating the regression model during gait. Such an approach could allow the system to adapt to changing environments, reduce the amount of training required to build the models, and improve session to session robustness since the models would be constructed as the subject walked.

The key limitation of our experimental study was that we only examined estimator performance during steady state, level walking on a treadmill in the gait lab. In order to successfully implement the estimation techniques outside of the lab, modes such as overground walking, ramp walking, and stair ascent/descent must also be addressed. One approach would be to generate individual models for each mode and apply a methodology to switch between them. We will address these issues in future work.

VI. Conclusion

Accurate state estimates allow a powered AFO to adapt to changing environmental and functional needs. In contrast to previous methods of state estimation that rely largely on thresholding sensor measurements, this paper presented a method of state estimation based on CC between a window of past sensor measurements and a learned model. This approach—along with three others for comparison—was implemented on a powered AFO. Experiments with healthy and impaired subjects suggested that our CC state estimator provided the best overall performance.

Acknowledgment

The authors would like to thank E. Morris and the investigators in the Comparative Neuromechanics Laboratory at Georgia Institute of Technology (Prof. Y.-H. Chang, M. Toney, and J. Yen) for their assistance.

References

[1] J. Perry, *Gait Analysis: Normal and Pathological Function*. Thorofare, NJ: Slack Inc., 1992.

[2] R. R. Neptune, S. A. Kautz, and F. E. Zajac, "Contributions of the individual ankle plantar flexors to support, forward progression and swing initiation during walking," *J. Biomech.*, vol. 34, no. 11, pp. 1387–1398, Nov. 2001.

[3] D. A. Winter, *Biomechanics and Motor Control of Human Movement*. Hoboken, NJ: Wiley, 2005.

[4] A. M. Dollar and H. Herr, "Lower extremity exoskeletons and active orthoses: Challenges and state-of-the-art," *IEEE Trans. Robot.*, vol. 24, no. 1, pp. 144–158, Feb. 2008.

[5] T. M. Becker Orthopedic, "Becker orthopedic," Online Catalog, 2009.

[6] S. Yamamoto, M. Ebina, M. Iwasaki, S. Kubo, H. Kawai, and T. Hayashi, "Comparative study of mechanical characteristics of plastic AFOs," *J. Prosthet. Orthot.*, vol. 5, no. 2, pp. 59–64, 1993.

[7] H. B. Kitaoka, X. M. Crevoisier, K. Harbst, D. Hansen, B. Kotajarvi, and K. Kaufman, "The effect of custom-made braces for the ankle and hindfoot on ankle and foot kinematics and ground reaction forces," *Arch. Phys. Med. Rehabil.*, vol. 87, no. 1, pp. 130–135, 2006.

[8] G. K. Rose, *Orthotics: Principles and Practice*. London, U.K.: Heinemann, 1986.

[9] W. Svensson and U. Holmberg, "Ankle-foot-orthosis control in inclinations and stairs," in *Proc. IEEE Conf. Robot., Autom. Mechatronics*, 2008, pp. 301–306.

[10] J. A. Blaya and H. Herr, "Adaptive control of a variable-impedance ankle-foot orthosis to assist drop-foot gait," *IEEE Trans. Neural Syst. Rehabil. Eng.*, vol. 12, no. 1, pp. 24–31, Mar. 2004.

[11] A. W. Boehler, K. W. Hollander, T. G. Sugar, and D. Shin, "Design, implementation and test results of a robust control method for a powered ankle foot orthosis (AFO)," in *Proc. Int. Conf. Robot. Autom.*, 2008, pp. 2025–2030.

[12] J. Furusho, T. Kikuchi, M. Tokuda, T. Kakehashi, K. Ikeda, S. Morimoto, Y. Hashimoto, H. Tomiyama, A. Nakagawa, and Y. Akazawa, "Development of shear type compact MR brake for the intelligent ankle-foot orthosis and its control," in *Proc. Int. Conf. Rehabil. Robot.*, 2007, pp. 89–94.

[13] C. M. Kim and J. J. Eng, "The relationship of lower-extremity muscle torque to locomotor performance in people with stroke," *Phys. Ther.*, vol. 83, no. 1, pp. 49–57, 2003.

[14] D. J. Weber, R. B. Stein, K. M. Chan, G. Loeb, F. Richmond, R. Rolf, K. James, and S. L. Chong, "Bionic walkaide for correcting foot drop," *IEEE Trans. Neural Syst. Rehabil. Eng.*, vol. 13, no. 2, pp. 242–246, Jun. 2005.

[15] K. W. Hollander, R. Ilg, T. G. Sugar, and D. Herring, "An efficient robotic tendon for gait assistance," *J. Biomech. Eng.*, vol. 128, no. 5, pp. 788–791, 2006.

[16] J. Hitt, A. M. Oymagil, T. Sugar, K. Hollander, A. Boehler, and J. Fleeger, "Dynamically controlled ankle-foot orthosis (DCO) with regenerative kinetics: Incrementally attaining user portability," in *Proc. Int. Conf. Robot. Autom.*, Apr. 10–14, 2007, pp. 1541–1546.

[17] J. M. Hausdorff and H. Ring, "Effects of a new radio frequency-controlled neuroprosthesis on gait symmetry and rhythmicity in patients with chronic hemiparesis," *Amer. J. Phys. Med. Rehabil.*, vol. 87, no. 1, pp. 4–13, 2008.

[18] K. A. Shorter, E. T. Hsiao-Wecksler, G. F. Kogler, E. Loth, and W. K. Durfee, "A portable-powered-ankle-foot-orthosis for rehabilitation," *J. Rehabil. Res. Dev.*, vol. 48, pp. 459–472, 2010.

[19] A. Forner-Cordero, H. J. F. M. Koopman, and F. C. T. van der Helm, "Describing gait as a sequence of states," *J. Biomech.*, vol. 39, no. 5, pp. 948–957, 2006.

[20] A. V. Oppenheim and R. W. Schafer, *Digital Signal Processing*. Upper Saddle River, NJ: Prentice-Hall, 1975.

[21] R. T. Collins, R. Gross, and J. Shi, "Silhouette-based human identification from body shape and gait," in *Proc. 5th IEEE Int. Conf. Automat. Face Gest. Recognit.*, 2002, pp. 366–371.

[22] J. Mantyjarvi, M. Lindholm, E. Vildjiounaite, S. M. Makela, and H. A. Ailisto, "Identifying users of portable devices from gait pattern with accelerometers," in *Proc. Int. Conf. Acoust., Speech, Signal Process.*, 2005, vol. 2, pp. 973–976.

[23] R. Kram, T. M. Griffin, J. M. Donelan, and Y. H. Chang, "Force treadmill for measuring vertical and horizontal ground reaction forces," *J. Appl. Physiol.*, vol. 85, no. 2, pp. 764–769, 1998.

[24] W. S. Cleveland and S. J. Devlin, "Locally weighted regression: An approach to regression analysis by local fitting," *J. Amer. Stat. Assoc.*, vol. 83, no. 403, pp. 596–610, 1988.

[25] C. M. Bishop, *Pattern Recognition and Machine Learning*. New York: Springer-Verlag, 2006.

[26] D. P. Ferris, K. E. Gordon, G. S. Sawicki, and A. Peethambaran, "An improved powered ankle-foot orthosis using proportional myoelectric control," *Gait Posture*, vol. 23, no. 4, pp. 425–428, 2006.

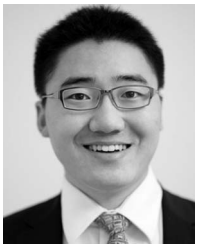

David Yifan Li (S'11) received the B.S. degree from Tsinghua University, Beijing, China, in 2007, and the M.S. degree from the University of Illinois at Urbana-Champaign, Urbana, in 2009.

He is currently involved in the human assist device test bed at the Center for Compact and Efficient Fluid Power, MN. His research interests include human gait analysis and pneumatic and hydraulic powered orthotic/prosthetic devices motion control and its energy efficiency enhancement.

Aaron Becker (S'06) received the B.S. degree in computer engineering from Iowa State University, Ames, and the M.S. degree in electrical and computer engineering from the University of Illinois at Urbana-Champaign, Urbana.

He is currently with the Department of Electrical and Computer Engineering, University of Illinois at Urbana-Champaign, where he is involved in studies of controllability and observability for robotics applications. These include powered orthotics, steering massively under-actuated mobile robotic ensembles, and minimal sensing applications in field robotics.

Kenneth Alex Shorter received the B.S. degree from the University of Colorado, Boulder, in 2001, and the M.S. and Ph.D. degrees from the University of Illinois at Urbana-Champaign, Urbana, in 2007 and 2011, respectively, all in mechanical engineering.

He currently holds a Postdoctoral Fellowship at the Woods Hole Oceanographic Institution, Woods Hole, MA. After completing his postdoctoral research, he will shortly join the Department of Mechanical Engineering, University of Michigan, Ann Arbor, as a Research Investigator, in Fall 2011. His research interests include gait analysis, musculoskeletal biomechanics, assistive device design, and the design and use of biologging devices for the study of animal behavior, physiology, and ecology.

Timothy Bretl (S'02–M'05) received the B.S. degree in engineering and the B.A. degree in mathematics from Swarthmore College, Swarthmore, PA, in 1999, and the M.S. and Ph.D. degrees in aeronautics and astronautics from Stanford University, Stanford, CA, in 2000 and 2005, respectively.

Subsequently, he was a Postdoctoral Fellow in the Department of Computer Science, Stanford University. Since 2006, he has been an Assistant Professor in the Department of Aerospace Engineering and a Research Assistant Professor in the Coordinated Science Laboratory at the University of Illinois at Urbana-Champaign, Urbana. His current research interests include the intersection of robotics and neuroscience.

Elizabeth T. Hsiao-Wecksler (M'10) received the B.S. degree from Cornell University, Ithaca, NY, the M.S. degree from Rochester Institute of Technology, Henrietta, NY, and the Ph.D. degree from the University of California, Berkeley.

She held a Postdoctoral Fellowship in the Integrated Rehabilitation Engineering Program at Boston University and Harvard Medical School. She is a Faculty Member in the Department of Mechanical Science and Engineering, University of Illinois at Urbana-Champaign, Urbana. She directs the Human Dynamics and Controls Laboratory. Her research interests include locomotion musculoskeletal biomechanics and assistive device design.